

This is the peer reviewed version of the following article:

Modeling and optimization of industrial internal combustion engines running on Diesel/syngas blends / Rinaldini, Carlo Alberto; Allesina, Giulio; Pedrazzi, Simone; Mattarelli, Enrico; Tartarini, Paolo. - In: ENERGY CONVERSION AND MANAGEMENT. - ISSN 0196-8904. - 182:(2019), pp. 89-94. [10.1016/j.enconman.2018.12.070]

Terms of use:

The terms and conditions for the reuse of this version of the manuscript are specified in the publishing policy. For all terms of use and more information see the publisher's website.

02/05/2026 03:09

(Article begins on next page)

36 technologies for syngas production, biomass gasification is one of the most promising. Small scale
37 power plants generally rely on internal combustion engines for the final energy conversion of the
38 gaseous fuel into mechanical and then electrical power. The system complexity can range from simple
39 open top reactors to multi-stage gasifiers [4]. On a worldwide literature scale, Susastriawan et al. [5]
40 reviewed the most common technologies used for small scale gasification, while Patuzzi et al. focused
41 on the northern part of Italy [6]. The Compression Ignition (CI) engine is the most obvious candidate
42 for burning syngas, due to its intrinsic high efficiency and robustness [7]. When operated in dual fuel
43 (DF) mode, CI engines show a reduction of diesel oil fuel consumption and of particulate matter
44 emissions. This was observed in the experimental tests for syngas use in oleaginous-based power
45 plants [8], in syngas-Balanites aegyptiaca ester oil blends [9]. Effects of Diesel substitution were
46 observed also in single-cylinder engines [10]. In this work, a Kohler KDW 1404, 4-cylinder, indirect
47 injection engine is considered. The engine is modeled by means of a CFD-3D code (KIVA-3V), in
48 order to analyze the simultaneous combustion of diesel oil and syngas under several operating
49 conditions. The use of CFD allows for an in-depth sight of the combustion process revealing details
50 that cannot be easily measured with more expensive experimental tests. Moreover, numerical
51 simulations allows for the analysis of a large number of configurations and making reliable
52 comparisons thanks to the possibility of varying one parameter at the time while boundary conditions
53 are keep strictly constant. However, the engine model used in this work had been previously
54 calibrated on the base of experimental campaign results [8], where the engine was coupled to a
55 commercial fixed bed gasifier produced by All Power Labs (model PP10) [11]. As far as the CFD
56 analysis is concerned, particular attention is paid to the dual fuel combustion process, requiring the
57 modeling of a series of complex phenomena: liquid fuel injection, droplets atomization and
58 vaporization, mixing of Diesel vapor within the air-syngas premixed environment and ignition. For
59 the optimization of dual combustion, two fundamental parameters are varied: syngas-diesel share and
60 the Diesel injection advance. The choice of these two parameters is motivated by the possibility to
61 easily tune them in almost any type of Diesel engine, employed in stationary applications. Starting
62 from a previously validated standard diesel combustion model, a flame propagation model was
63 implemented and added to simulate the combustion process in a dual fuel regime. Results show a
64 strong dependence of combustion patterns on the share of energy substitution from Diesel oil to
65 syngas. At some operating points, the syngas-supported combustion enables a noticeable increase of
66 engine brake efficiency. On the other hand, an excess of syngas leads to undesired high values of peak
67 pressure within the combustion chamber. The CFD simulation results provide a comprehensive
68 overview on the influence of both the start of injection angle (SOI) and the share of syngas. Assuming
69 a maximum peak cylinder pressure value of 100 bar, a correlation between the optimum SOI and the
70 share of syngas is extrapolated. Obviously, the optimum SOI corresponds to the maximum brake
71 efficiency of the engine, while complying with the constraint on combustion pressure. The limit of
72 100 bar is based on the authors experience, as well as on the results of a previous comprehensive

73 experimental campaign on the same Kohler engine running on standard Diesel oil. The measured
74 parameters are also employed as a reference for the calibration of the CFD-3D engine model.
75 Particular attention is obviously paid to the combustion process. The calibrated model is then applied
76 to the investigation of a broad range of operating conditions in order to map the effects of combined
77 variations of syngas-Diesel share and start of injection timing. The use of CFD analysis allows to
78 investigate conditions where the peak pressure may exceed the maximum value suggested by the
79 engine manufacturer.

80

81 **2 MATERIALS AND METHODS**

82

83 Compression ignition engines always require a minimum amount of Diesel fuel, in order to inject the
84 premixed air-syngas charge. In many cases, the substitution rates can be pushed up to 90-95% [12],
85 however in this work the substitution range is limited to 60% of the fuel total chemical energy. A
86 further increase was experimentally demonstrated to produce unacceptable peaks of cylinder gas
87 pressures (over 150 bar), therefore the 60% limit was set in order to preserve the mechanical integrity
88 of the engine.

89

90

91 **2.1 Gasification and engine facility**

92

93 The syngas composition input used in the modeling of the systems derives from the analysis of the
94 producer gas obtained during the experimental tests that lead also to model calibration. During the
95 experimental campaign, the Kohler KDW 1404 engine was connected to a gasification unit model
96 Power Pallet PP10 manufactured by All Power Labs [11]. The Power Pallet is a complete power-
97 delivery system equipped with a gas generation reactor, a filtration stage composed of a cyclone and a
98 woodchips packed-bed drum filter and an engine-generator unit that consists in a model DG972 3-
99 cylinder Kubota engine. For the experimental run the whole generator unit was disconnected and the
100 filtered gas directly sent to the compression ignition engine instead. The gasification reactor is a fixed
101 bed, single throat, Imbert-type gasifier fed from the top through an auger connected to a 63 liters fuel-
102 storage hopper. For the experimental campaign dry poplar wood chips were used as fuel. After a start-
103 up period of about 20 minutes where the gas was burned in a flare, the gas composition resulted stable
104 with little or no dependency on the flow rate required by the engine. This feature characterizes the
105 Imbert-type gasifiers, it was vital in the past for variable load application such as vehicle propulsion,
106 and it is known in classic literature as ‘turn down ratio’ as reported in the FAO “Wood Gas as an
107 Engine Fuel” book [13] and in the Reed’s gasification handbook [14]. The gasification facility
108 description, as reported by the manufacturer, is summarized in Table 1. During the tests the gasifier
109 behavior was proven to be stable, combustion temperature set itself to 920 °C, while the temperature

110 at the end of the reduction zone was 770 °C. The composition analysis of the produced gas was
 111 performed through two tests run in a Pollution 3000 Micro-GC gas analyzer. The lower heating value
 112 of the syngas is calculated as follows:

$$113 \quad LHV_{syngas} = LHV_{H_2}x_{H_2} + LHV_{CO}x_{CO} + LHV_{CH_4}x_{CH_4} \quad (1)$$

114
 115 where LHV_{syngas} [MJ/Nm³] is the syngas lower heating value; LHV_{H_2} [MJ/Nm³] is the hydrogen lower
 116 heating value (10.8 MJ/Nm³ [15]); x_{H_2} [% mol] is hydrogen molar fraction in the syngas; LHV_{CO}
 117 [MJ/Nm³] is the carbon monoxide lower heating value (12.6 MJ/Nm³ [15]); x_{CO} [% mol] is carbon
 118 monoxide molar fraction in the syngas; LHV_{CH_4} [MJ/Nm³] is the methane lower heating value (35.9
 119 MJ/Nm³ [15]) and x_{CH_4} [% mol] is methane molar fraction in the syngas. About the IC engine, a 4-
 120 cylinder Kohler KDW 1404, with indirect injection [16] was used in an engine test bench described
 121 by the authors [8]. Some engine features reported in Table 2 indicate the highly robustness and
 122 reliability of this engine, which is normally used in industrial and agricultural applications.

123

124

Table 1 APL PP10 features [11].

Parameter	Value
Power output	from 3 to 10 kW electrical power
Maximum biomass consumption	12 kg/h @ 10 kWel
Fuel moisture tolerance	up to 30% moisture content
Dimensions (LxWxH)	1.2 x 1.2 x 1.8 m
Weight	499 kg

125

126

Table 2 Kohler KDW 1404 features [16]

Parameter	Value
Cylinders	4-in line
Total displacement	1372 cm ³
Bore	75 mm
Stroke	77.6 mm
Compression ratio	22.8:1
Injection system	Indirect injection with injector dump on head
Applications	Excavator, dumper, roller, generation set

127

128

129

130

131 2.2 Gas flow rate measurement and control

132

133 During the calibration tests the engine run under two different conditions in terms of syngas-Diesel
 134 share. Unlike other systems on the market where an air blower push air into the reactor to generate a
 135 specific amount of gas, the system chosen works below atmospheric pressure. It is the engine that
 136 draws gas from the reactor and through the filtration stage. For the calibration tests the same
 137 architecture of the original generator was used: the diesel engine air intake was connected to the
 138 reactor using a tee as shown in Figure 1. Due to the pressure drop generated by the gasifier-filter
 139 system, air will always find its way into the open branch of the tee. For this reason, acting on the air
 140 valve placed in this branch, the engine is forced to draw both gas and air. A differential pressure
 141 meter, connected to a calibrated orifice in the gas branch keeps records of the gas flow rate thanks to
 142 the following equation:

143

$$144 \quad Q_m = \frac{C}{\sqrt{1-\beta^4}} \varepsilon \frac{\pi d^2}{4} \sqrt{2\rho_l \Delta p} \quad (2)$$

145 where C is the coefficient of discharge, β is the ratio between the pipe and the orifice diameters, d is
 146 the orifice diameter, ρ_l is the fluid density, as function of the temperature, ΔT is the differential
 147 pressure across the plate, ε is the expansibility factor, calculated as follows:

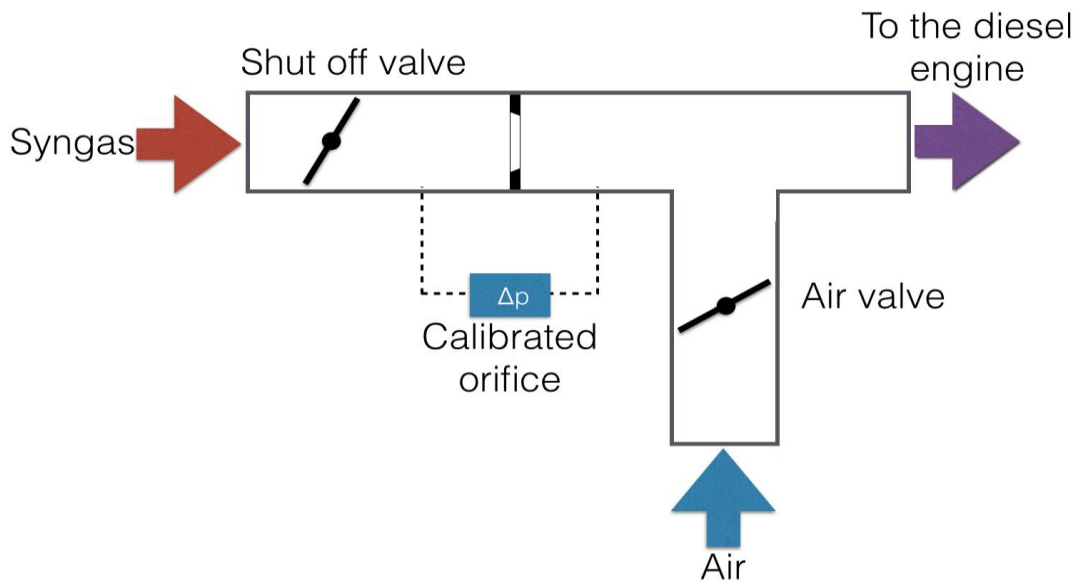
148

$$149 \quad \varepsilon = 1 - (0.41 + 0.35\beta^4) \frac{\Delta p}{k \cdot p_l} \quad (3)$$

150

151 where k is the heat capacity ratio, p_l is the upstream pressure.

152



153

154 **Figure 1** Syngas-air mixing system (adapted from [8])

155
156 **2.3 Computational Fluid Dynamic Model**

157
158 The CFD model used in this work is based on the KIVA-3V code, customized for the purposes of the
159 study. In particular, a specific chemical kinetic sub-model is implemented for the investigation of the
160 syngas-diesel dual fuel (DF) operations. A list of the most important sub-models employed in the
161 customized version of the KIVA 3V code is shown in Table 3.

162
163 **Table 3** Description of the modeling environment

Modeling Environment	Description
Turbulence model	RNG k-H
model Breakup	model Hybrid KH-RT
model Droplet collision	model Droplet trajectories
Evaporation model	Single component, KIVA-3V
Diesel Combustion	PaSR / coupled chemical kinetics
Flame Propagation	TFC / Premix code for aspirated fuel
Fuel composition	Syngas/DOS

164
165 Most of the sub-models mentioned in Table 3 were widely used by the authors within KIVA-3V and
166 KIVA 4 environments, so a detailed description of their implementation can be found in previous
167 works. For example, Mattarelli et al. [17] applied the KIVA CFD model to light duty Dual Fuel
168 (Diesel/Natural Gas) combustion engine. The model is able to predict the emission formation as
169 reported by Golovitchev et al. [18]. In addition, the model was used to simulate 2-stroke engines [19]
170 and Miller cycle diesel engine [20]. The present paper only reviews the modeling of syngas-Diesel
171 simultaneous combustion. This goal is achieved thanks to the synergy between two different sub-
172 models. The first one, typically employed for standard Diesel operations, is the partially premixed
173 reactor spray combustion model, PaSR, [21]; the second is a specific flame propagation model. For
174 the latter, the authors implemented a new expression for the reaction rate. The development and
175 validation of the chemical kinetic mechanisms were carried out with the support of experiments:
176 ignition delay times measured in shock tubes, for different natural gas/diesel premixed charge
177 compositions and flame propagation data for the main constituent components of natural gas. The

178 mechanism tuning methodology used in this study was based on a sensitivity analysis of complex
179 mechanisms and it is comprehensively described in [22].

180 Before the investigation on the Dual Fuel operations, a CFD-3D model of the engine cylinder was
181 built and validated by comparison with experimental data, for both Normal Diesel (ND) and Diesel-
182 syngas Dual Fuel (DF) combustion. The computational grid cannot be shown due to not-disclosure
183 agreements; it was generated to accurately reproduce the geometric details of the combustion
184 chamber, to achieve the actual compression ratio and to get a good aspect ratio of cells. The typical
185 cell size is about 0.5-1.0 mm and a minimum of 4 cell layers was enforced in the squish region at Top
186 Dead Center. As demonstrated in previous analyses [18], experimentally validated in [23], these
187 meshing criteria guarantee a good compromise between accuracy and computational demand. The
188 computational grid consists of about 100,000 cells at BDC and of about 20,000 at TDC.

189 Initial conditions for combustion simulations, such as pressure, temperature, trapped mass and charge
190 composition, were obtained from experimental data, while in-cylinder initial velocity was imposed on
191 the basis of the authors' experience. However, this arbitrary hypothesis should have a negligible
192 influence on combustion, since the hyper turbulence imparted by the pre-chamber is supposed to
193 prevail on any variation of the in-cylinder initial flow field.

194

195 **3 RESULTS AND DISCUSSION**

196

197 Both experimental and CFD results show a strong dependence on engine in-cylinder pressure and
198 overall efficiency on the share of Diesel substitution.

199

200 **3.1 Calibration tests**

201

202 Syngas sampling results are reported in Table 4. Data show a negligible variability among the
203 samples. The calculated average gas composition is 6 MJ/Nm³. This value is in agreement with the
204 recorded behavior of downdraft fixed bed reactors [3,4].

205

206

Table 4 Syngas composition

	x_{H_2}	x_{N_2}	x_{CH_4}	x_{CO}	x_{CO_2}	LHV_{syngas}
	[% mol.]	[% mol.]	[% mol.]	[% mol.]	[% mol.]	[MJ/Nm ³]
Sample 1	20.3	45.2	1.8	25.0	7.6	5.99
Sample 2	20.3	45.3	1.8	25.1	7.5	6.00
Average	20.3	45.3	1.8	25.1	7.6	6.00

207
 208
 209
 210
 211
 212
 213
 214
 215
 216
 217
 218
 219

Combustion simulation results were compared to experiments for 2 operating points: the first is an ND operation, full load, 3000 rpm and the second was derived from the first, reducing the injected Diesel fuel of about 38% and replacing it with the amount of syngas that enables the engine to generate the same brake power. Table 5 reports the details of each operating point while Figure 2 shows the comparison between predicted and measured in-cylinder pressure. As visible, for both ND and DF operations, close agreement with experiments was found. From the data in Table 4 and from Figure 2, it can be also seen that DF combustion yields a slight increase of engine brake efficiency (+2.3%) but also leads to an increment in in-cylinder peak pressure (about 8 bar). The same tendency was observed in a previous work by Rinaldini et al. [2], where a Common Rail 2.8 liter, turbocharged Diesel engine, fueled by both syngas and Diesel, was tested at the dynamometer bench. Here, a slightly higher brake efficiency increment of 5 % was measured at a diesel substitution rate of 27 %

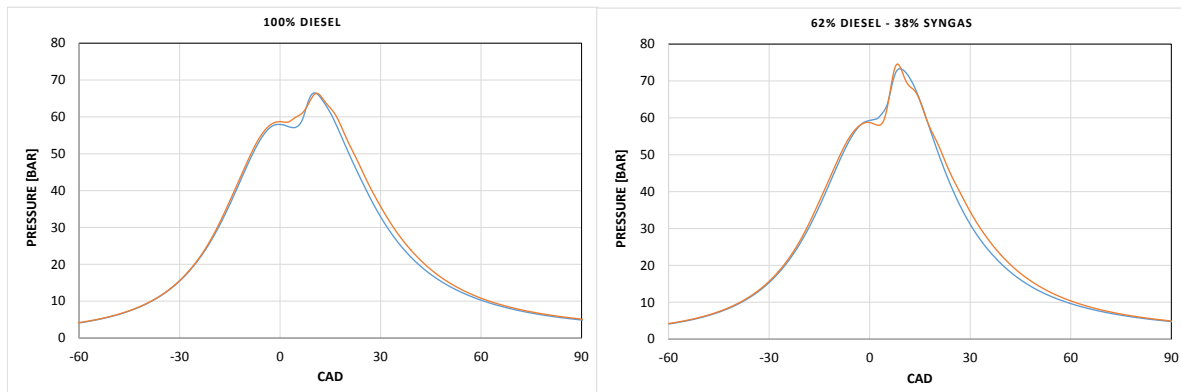


Figure 2 Model Validation

220
 221
 222
 223

Table 5 Engine operating point used for the model validation

		ND	DF
Rotational speed	rpm	3000	3000
Power	kW	15.65	15.65
Diesel flow rate	l/h	5.40	3.35
Diesel fuel power	kW	54.45	33.78
Syngas flow rate	Nm ³ /h	0.00	11.67
Syngas fuel power	kW	0.00	19.45

224 3.2 Model results

225

226 In order to analyze DF combustion, a set of CFD-3D simulations were performed, by using the
 227 calibrated models and varying both syngas premixed concentration and Diesel injection strategies. In
 228 detail, the amount of injected Diesel fuel was progressively reduced and substituted with premixed
 229 syngas; for each DF simulated case, the amount of syngas was calculated, according to Eq. 4, in order
 230 to keep the ND case equal to the total amount of energy introduced with the two fuels. The Diesel
 231 Replacement Rate (DRR) parameter, defined in Eq. 5, was used to identify the substitution levels.
 232 Finally, the Start of Injection (SOI) of Diesel fuel (-4 CAD ATDC for base engine) was varied from -
 233 8 CAD ATDC to 2 CAD ATDC.

234

$$235 \quad m_{syngas,DF} = (m_{Diesel,ND}k_{i,Diesel} - m_{Diesel,DF}k_{i,Diesel})/k_{i,syngas} \quad (4)$$

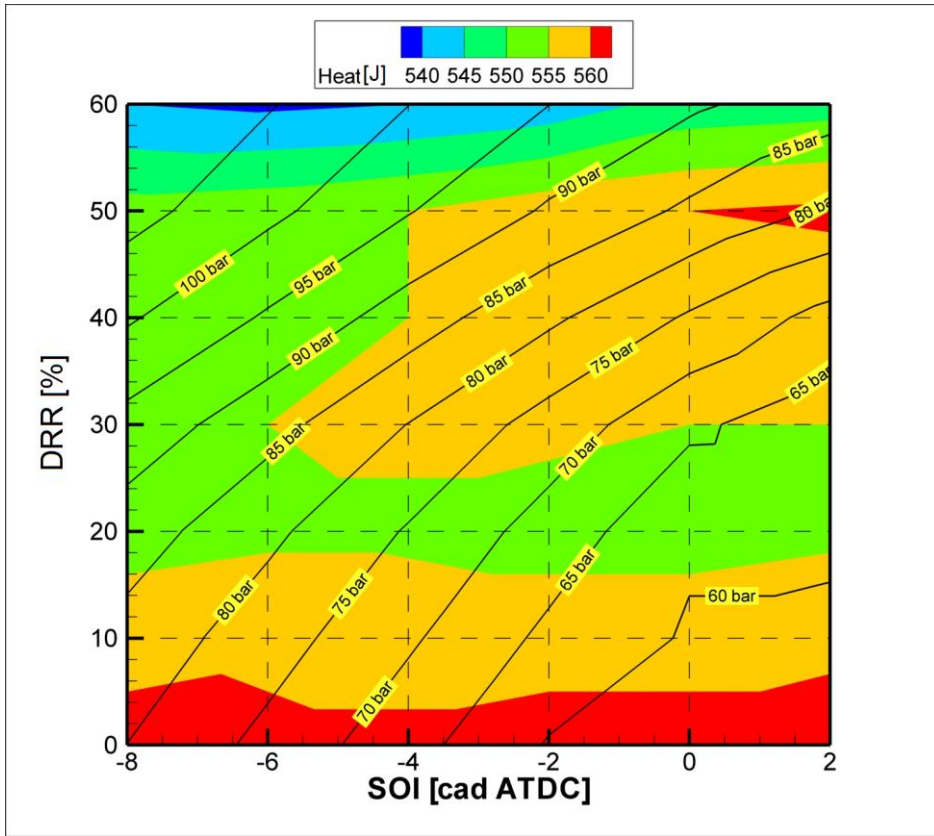
236

$$237 \quad DRR = (m_{Diesel,ND} - m_{Diesel,DF})/m_{Diesel,ND} \quad (5)$$

238

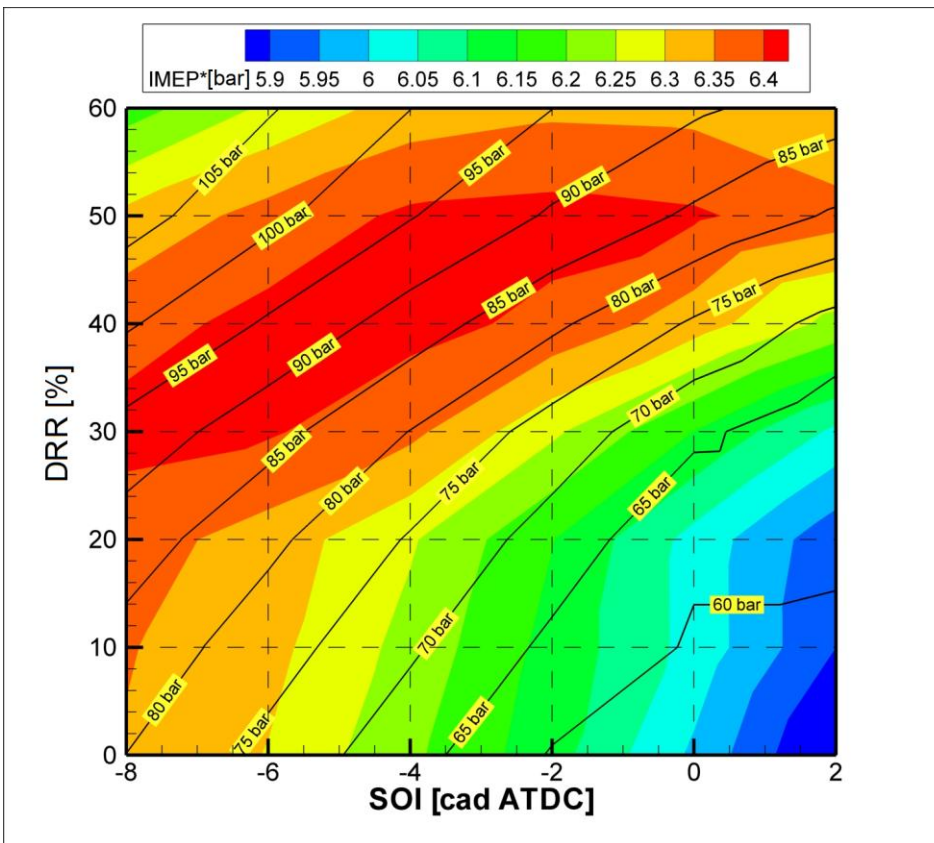
239 In order to evaluate the indicated work, directly related to the engine power output, the Gross
 240 Indicated Mean Effective Pressure (IMEP*) is calculated as the pressure-volume integral from -60° to
 241 110° after firing TDC, divided by the engine unit displacement. Figures 3 and 4 are the maps of total
 242 heat released by combustion and IMEP*; these parameters are plotted as a function of the syngas
 243 fraction (corresponding to DRR) and start of injection (SOI). The solid lines crossing the maps
 244 represent the iso-values of maximum in-cylinder pressure, reached for each combination of DRR and
 245 SOI. It is important to notice that these results cannot be directly compared to the ones previously
 246 presented for the model validation, since they are obtained under different conditions (same engine
 247 power output for the calibration results, same fuel input energy for the current ones).

248



249
250
251

Figure 3 Modeled combustion heat release Vs. DRR and SOI



252
253

Figure 4 Modeled IMEP* Vs. DRR and SOI

254 Looking at Figure 3 and 4, the following considerations can be made.

- 255 ● Combustion heat release slightly decreases as DRR increases; however, variations are quite
256 small (max 4%), indicating that combustion efficiency is more or less the same over the map.
257 As a result, engine indicated efficiency depends almost entirely on the efficiency of the
258 conversion of heat into work: therefore, the higher is IMEP*, the higher will be the engine
259 fuel conversion efficiency.
- 260 ● As expected, earlier injections correspond to larger IMEP* but also to higher in-cylinder
261 pressures (in-cylinder peak pressure iso-lines and IMEP* bands have approximately the same
262 shape); moreover, as DRR increases, IMEP* and peak pressures increase.
- 263 ● Considering a limit for peak cylinder pressure of 100 bar, it may be observed from figure 4
264 that any rate of substitution from 10 to 60% can yield a value of IMEP* higher than in the ND
265 operation, while complying with the above mentioned constraint. This means that dual fuel
266 operations may improve the brake performance and efficiency of the engine (1-5%), without
267 drawbacks in terms of mechanical stress on the cylinder components.
- 268 ● For DRR higher than 50%, there is a drop in the IMEP* values, even if the in-cylinder peak
269 pressure continues to increase: a possible explanation for this result may be the slight
270 reduction of combustion efficiency, demonstrated in Figure 3 by the fall of released heat.

271

272 **3.3 Optimization of the engine brake efficiency**

273

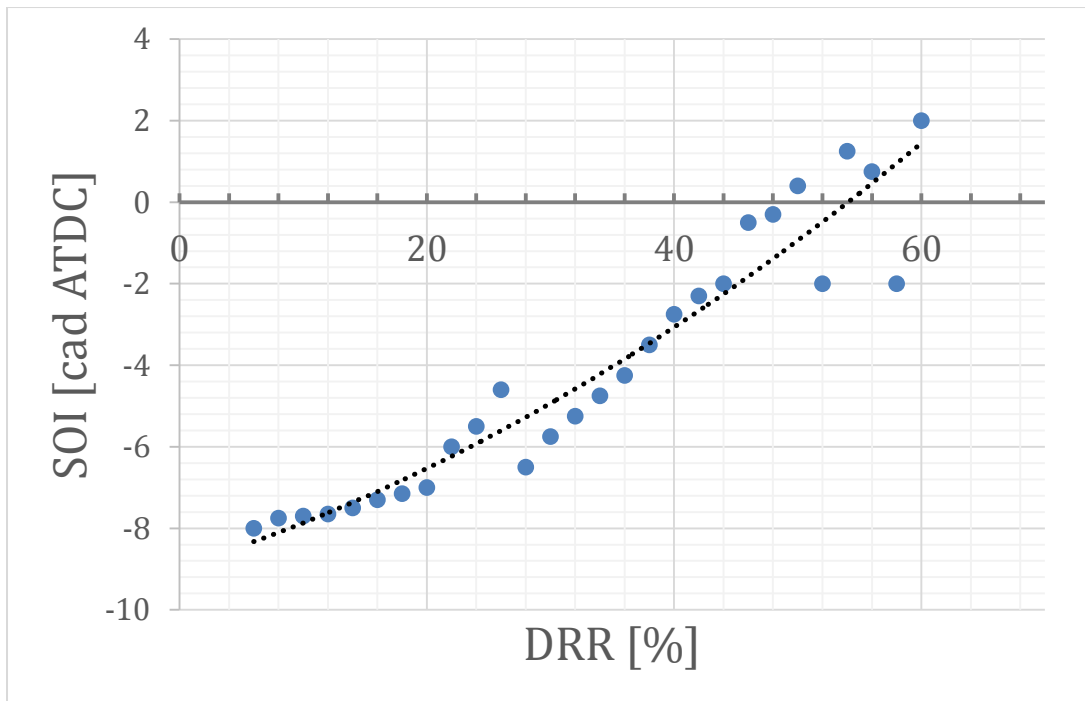
274 From the analysis of figures 4 and 5 it is also possible to determine a correlation between the Diesel
275 substitution rate (DRR), and the SOI angle, that maximizes the engine brake efficiency, while
276 complying with the above mentioned limit of 100 bar for the peak cylinder pressure. For the same
277 level of efficiency, the SOI angle that provides minimum cylinder pressure was chosen. The results of
278 this post-processing activity are presented in figure 5. For this set of data, a second degree polynomial
279 interpolation curve was calculated:

280

$$281 \text{SOI [cad ATDC]} = 0.0013\text{DRR}^2 + 0.094\text{DRR} - 8.9406 \quad (6)$$

282

283 The coefficient of determination (R^2) is 0.9134. The scattering of points in Figure 5 that does not
284 allow the definition of a higher degree polynomial monotonic function. Eq. 6 can be used as a basis
285 for defining the injection strategy of all the engines of the same type, simultaneously operating with
286 syngas and Diesel.



287
288 **Figure 5** SOI-DRR correlation for maximizing engine brake efficiency
289

290 **4 CONCLUSIONS**

291
292 A CFD-3D combustion analysis of a 1.4 liter, 4-cylinder, IDI industrial Diesel engine was carried out,
293 using a KIVA-3V model, validated by experiments. Two types of combustion were investigated: a
294 conventional Diesel combustion (ND), and a dual fuel (DF) combustion, where the Diesel fuel is
295 partially replaced by syngas. The maximum rate of substitution considered in the study is 60%. The
296 main goal of the study was to analyze the influence of the injection strategy, as well as to assess the
297 potential of this dual fuel combustion in terms of engine performance and brake efficiency.

298 It was found that for substitution rates up to 40-50% engine performance and efficiency can increase a
299 little bit (1-5%), however it is fundamental to properly set the injection angle, in order to control peak
300 cylinder pressure. In order to achieve the maximum fuel efficiency, while complying with the
301 pressure limit, a correlation between optimum SOI and the replacement rate was calculated. This
302 function can be applied also to different engines, of the same type. Dual fuel combustion of Diesel
303 and syngas was demonstrated to be an effective way to exploit renewable energy sources, with
304 minimum modifications to the existing engines.

310 **Nomenclature**

Acronym/abbreviation	Meaning
ATDC	After Top Dead Center
BDC	Bottom Dead Center
CAD	Crankshaft Angle Degrees
CFD	Computational Fluid Dynamics
CI	Compression Ignition
DF	Dual Fuel
DOS	Diesel Oil Surrogate
DRR	Diesel replacement rate
IC	Internal Combustion
IMEP	Indicated Mean Effective Pressure
KH-RT	Kelvin-Helmholtz Rayleigh-Taylor
LHV	Lower Heating Value
ND	Normal Diesel
PaSR	Partially Stirred Reactor
RNG	Renormalization Group
SOI	Start Of Injection
TDC	Top Dead Center
TFC	Turbulent Flame Closure

311

312 **References**

313

314 [1] OECD/IEA. Technology Roadmap - Delivering Sustainable Bioenergy,
 315 [http://www.iea.org/publications/freepublications/publication/Technology_Roadmap_Delivering_Sust](http://www.iea.org/publications/freepublications/publication/Technology_Roadmap_Delivering_Sustainable_Bioenergy.pdf)
 316 [ainable_Bioenergy.pdf](http://www.iea.org/publications/freepublications/publication/Technology_Roadmap_Delivering_Sustainable_Bioenergy.pdf) [accessed 25 October 2018].

317 [2] Rinaldini CA, Allesina G, Pedrazzi S, Mattarelli E, Savioli T, Morselli N, Puglia M, Tartarini P.
 318 Experimental investigation on a Common Rail Diesel engine partially fuelled by syngas. Energy
 319 Conversion and Management 2017;138:526-537. <https://doi.org/10.1016/j.enconman.2017.02.034>.

320 [3] Basu P. Biomass Gasification, Pyrolysis and Torrefaction, Pratical Design and Theory. 3rd ed.
 321 London: Academic Press; 2018.

322 [4] De Sales CAVB, Maya DMY, Lora EES, Jaén RL, Reyes AMM, González AM, Andrade RV,
 323 Martínez JD. Experimental study on biomass (eucalyptus spp.) gasification in a two-stage downdraft
 324 reactor by using mixtures of air, saturated steam and oxygen as gasifying agents. Energy Conversion
 325 and Management 2017;145:314-323. <https://doi.org/10.1016/j.enconman.2017.04.101>.

326 [5] Susastriawan AAP, Saptoadi H, Purnomo. Small-scale downdraft gasifiers for biomass
327 gasification: A review. *Renewable and Sustainable Energy Reviews* 2017; 76:989-1003.
328 <https://doi.org/10.1016/j.rser.2017.03.112>.

329 [6] Patuzzi F, Prando D, Vakalis S, Rizzo AM, Chiamonti D, Tirler W, Mimmo T, Gasparella A,
330 Marco Baratieri. Small-scale biomass gasification CHP systems: Comparative performance
331 assessment and monitoring experiences in South Tyrol (Italy). *Energy* 2016;112:285-293.
332 <https://doi.org/10.1016/j.energy.2016.06.077>.

333 [7] Dasappa S, Sridhar HV. Performance of a diesel engine in a dual fuel mode using producer gas
334 for electricity power generation, *International Journal of Sustainable Energy* 2013;32,3:153-168.
335 <https://doi.org/10.1080/14786451.2011.605945>.

336 [8] Allesina G, Pedrazzi S, Rinaldini CA, Savioli T, Morselli N, Mattarelli E, Tartarini P.
337 Experimental-analytical evaluation of sustainable syngas biodiesel CHP systems based on oleaginous
338 crop rotation (Conference Paper). In: *International conference on power engineering, ICOPE 2015;*
339 *PACIFIC Yokohama Conference Center Yokohama; Japan; 30 November 2015 through 4 December*
340 *2015; Code 118770*.

341 [9] Deshmukh SJ, Bhuyar LB, Thakre SB. Investigation on performance and emission characteristics
342 of CI engine fuelled with producer gas and esters of Hingan (Balanites) oil in dual fuel mode.
343 *International Journal of Aerospace and Mechanical Engineering* 2008;2,3:148-153.

344 [10] Mahgoub BKM, Sulaiman SA, Abdul Karim Za. Performance of a Compression Ignition Engine
345 Fuelled by Diesel and Imitated Syngas. *Asian Journal of Scientific Research* 2013;6: 456-466

346 [11] ALL Power Labs. PP10 Power Pallet datasheet, <http://www.allpowerlabs.com/> [accessed 25
347 October 2018].

348 [12] Kumar S, Date MA, Pandya RN, Patel S, Shah KC, Damour V, Jain BC. Design and
349 Development of a Biomass Based Small Gasifier-Engine System Suitable for Irrigational Needs in
350 Remote Areas of Developing Countries. In: *Energy from Biomass and Wastes VIII; Institute of Gas*
351 *Technology; Chicago; 1984*.

352 [13] United Food and Agriculture Organization. *Wood Gas as an Engine Fuel*. Rome: FAO Forestry
353 Paper; 1986.

354 [14] Reed TB, Das A. *Handbook of Biomass Downdraft Gasifier Engine Systems*. Golden
355 (Colorado): Solar Energy Research Institute;1984.

356 [15] The Engineering Toolbox. Gross and Net Heating Values for some common Gases, Available at:
357 https://www.engineeringtoolbox.com/gross-net-heating-values-d_420.html [accessed 25 October
358 2018].

359 [16] Kohler Power. KDW 1404 engine webpage, <http://www.kohlerpower.it/product/kdw-1404/>
360 [accessed 25 October 2018].

361 [17] Mattarelli E, Rinaldini CA, Golovitchev VI. CFD-3D analysis of a light duty Dual Fuel
362 (Diesel/Natural Gas) combustion engine. *Energy Procedia* 2014;45:929–37.
363 <https://doi.org/10.1016/j.egypro.2014.01.098>.

364 [18] Golovitchev VI, Rinaldini CA, Montorsi L, Rosetti A. CFD combustion and emission formation
365 modeling for a HSDI diesel engine using detailed chemistry. In: ASME 2006 Internal Combustion
366 Engine Division Fall Technical Conference; Sacramento, California; 5-8 November 2006;
367 <http://dx.doi.org/10.1115/ICEF2006-1506>.

368 [19] Mattarelli E, Rinaldini, CA, Cantore G. CFD optimization of a 2-stroke range extender engine.
369 *International Journal of Automotive Technology* 2015; 16 (3): 351-69.
370 <http://dx.doi.org/10.1007/s12239-015-0037-y>.

371 [20] Rinaldini CA, Mattarelli E, Golovitchev VI. Potential of the Miller cycle on a HSDI diesel
372 automotive engine. (2013) *Applied Energy* 2013;112:102-19.
373 <http://dx.doi.org/10.1016/j.apenergy.2013.05.056>.

374 [21] Golovitchev VI, Nordin N, Jarnicki R, Chomiak J. 3D Diesel Spray Simulation Using a New
375 Detailed Chemistry Turbulent Combustion Model. SAE Technical Paper 2000; No. 2000-01-1891.
376 <https://doi.org/10.4271/2000-01-1891>.

377 [22] Golovitchev VI, Imren A. Development of Dual Fuel Combustion Models for Direct Injected
378 Heavy Duty Diesel Engines. In: Silva C, Riveira A, editors. *Diesel Fuels: Characteristics,*
379 *Performances and Environmental Impacts*, New York:Nova Publisher; 2013

380 [23] Ehleskog, R, Golovitchev V, Denbratt I, Andersson S, Rinaldini CA. Experimental and
381 numerical investigation of split injections at low load in an HDDI diesel engine equipped with a piezo
382 injector. SAE Technical Papers 2006; No. 2006-01- 3433. <https://doi.org/10.4271/2006-01- 3433>.

383